



Pharmaceutical nanotechnology

Formulation and evaluation of cefuroxim loaded submicron particles for ophthalmic delivery



Gabriela Andrei^a, Cătălina A. Peptu^{a,*}, Marcel Popa^a, Jacques Desbrieres^b, Cristian Peptu^c, Fotios Gardikiotis^d, Marcel Costuleanu^d, Dănut Costin^d, Jean Charles Dupin^b, Arnaud Uhart^b, Bogdan I. Tamba^d

^a Gheorghe Asachi Technical University of Iasi, Department of Natural and Synthetic Polymers, Prof. dr. docent Dimitrie Mangeron street, Iasi 73, Romania

^b Université de Pau et des Pays de l'Adour, Institut des Sciences Analytiques et de Physico-Chimie pour l'Environnement et les Matériaux, IPREM, Hélioparc Pau Pyrénées, 2 Avenue P. Angot, Pau Cedex 09,64053 France

^c "Petru Poni" Institute of Macromolecular Chemistry, Aleea Grigore Ghica Voda 41A, Iasi 700487, Romania

^d "Grigore T. Popa" University of Medicine and Pharmacy, University Str., Iasi 16, Romania

ARTICLE INFO

Article history:

Received 16 April 2015

Received in revised form 16 July 2015

Accepted 17 July 2015

Available online 26 July 2015

Keywords:

Chitosan

Gelatin

Micro and nanoparticles

Cefuroxim

Ophthalmology

Drug delivery

ABSTRACT

Chitosan gelatin particles could be the ideal candidate for intraocular drug delivery due to their desirable properties. Double crosslinking in double emulsion has been used as an original and reliable method for particles preparation and their morphology has been optimized considering the main synthesis parameters such as polymers ratio, crosslinker amount, stirring speed, tensioactive amount and ionic crosslinking time, respectively. The particles have been analyzed for their physical–chemical properties (swelling degree, drug loading and release capacity, surface characteristics, etc.), the enzymatic degradation properties along with *in vivo* ocular investigations (ocular biodistribution, *in vivo* drug release). In the present study cefuroxim was used as a model drug, which is generally used in the prophylaxis of postoperative endophthalmitis following cataract surgery after intraocular administration. The present study proved that the dimensions and the physical–chemical properties of the particles can be modulated (by varying the preparation parameters) to facilitate the administration, the biodistribution and the drug release in the specific segment of the eye. This experimental study demonstrated also the ability of fluorescent nanoparticles to penetrate ocular tissues close to the administration site (intravitreal injection) and especially their tendency to migrate deep in the retina at time intervals of 72 h.

© 2015 Elsevier B.V. All rights reserved.

1. Introduction

The diseases of the posterior segment of the eye (glaucoma, diabetic retinopathy and age-related macular degeneration, etc.) are responsible for compromising eyesight of a large number of subjects. The therapeutic efficiency of pharmacological treatments in this area is limited mainly due to the difficulty of the active substance to reach the target tissues. That is the reason the delivery of therapeutic doses of drugs to the tissues in the posterior segment of the eye, however, represents a significant challenge. When a topical path is chosen, there are a lot of barriers (cornea, lens, haematoaqueous and haematoretinal barriers) which stop the medication access to the vitreous, the retina and the choroid.

On the other hand, if the oral pathway is selected, the amount of drug reaching the posterior segment of the eye coming from general blood flow is very low (Alarcón and Martínez, 2006). Also, therapeutic drug levels cannot be maintained for longer periods in target tissues.

In the last years, many pharmaceutical formulations have been used for the treatment of ocular diseases. Micro and nanotechnology ophthalmic formulations represent one of the approaches which are currently being designed for both anterior and posterior segment drug delivery. Several carriers, such as micro/nanoparticles, nanosuspensions, liposomes, nanomicelles and dendrimers have been developed for ocular drug delivery, some of them showing promising results for improving ocular bioavailability (Patel et al., 2013). Nanomicelles are carrier systems able to formulate therapeutic agents into clear aqueous solutions with high drug encapsulation efficiency. They are easy to prepare and present a small size and they have been proved to enhance the

* Corresponding author.

E-mail address: catipeptu@tuiasi.ro (C.A. Peptu).

monooleate–Tween 80 (Sigma–Aldrich); cefuroxim (CF) collagenase from *Clostridium histolyticum* (EC 3.4.24.3, US Biological, USA) with collagenase activity of 125 units/mg dry weight. All other chemicals used (solvents and other substances) were at least analytical grade.

2.2. Methods

2.2.1. Micro/nanocapsules preparation

Nano and microcapsules were obtained by two steps cross-linking of the two polymers (chitosan and gelatin) in a double emulsion system. The first step, represented by gelation through ionic crosslinking of the polymers solution was followed by a second step, covalent crosslinking, in order to harden the unstable gel particles.

Briefly, the procedure is the following: 0.25 g polymer mixture (depending on the sample) is dissolved in a specific amount of 1% acetic acid; afterwards, the amount of hydrophilic surfactant (Tween 80) is also dissolved. In order to prepare the primary emulsion, a certain amount of toluene (aqueous phase to organic phase ratio was 4/1) containing the specific surfactant, Span 80 has been dropped under vigorous stirring to the aqueous phase containing the two polymers. The primary emulsion has been added drop by drop into the organic phase (consisting in toluene and the certain amount of the hydrophobic surfactant—Span 80) under stirring at 9000–15,000 rpm. After 10 min the TPP solution was added also under stirring but only after the stirring speed was reduced at 5000 rpm (in order to ensure uniform ionic crosslinking and to diminish the aggregates formation due to the coalescence which can appear at a higher speed). The ionic crosslinking was allowed to take place for different time intervals (between 1 and 4 h). The following step was the addition of the covalent crosslinker (glutaraldehyde toluene solution) and left to react for 1 h. The micro and nanocapsules were separated by successive cycles of centrifugation—washing (with different solvents—acetone, water and finally hexane) and dried at room temperature.

As it is already known, the use of glutaraldehyde may increase the toxicity, thus limiting the possible medical applications of the prepared system. Therefore the neutralization of unreacted glutaraldehyde sites was performed as a supplementary step by treating the prepared nanoparticles repeatedly with L-glutamic acid solution (low pH) as reported by Goswami et al. (Goswami et al., 2010).

In order to establish the best formulation different parameters of both crosslinking reactions have been considered: the mass polymer ratio, TPP concentration, the molar ratio between the two polymers (in terms of free amine groups) and each of the two crosslinkers (TPP and GA), ionic crosslinking time, surfactant amount (in percent in respect with the aqueous or organic phase weight) and the stirring speed used at the beginning when the emulsion was formed. All the values of these parameters as well as the yields of each reaction are presented in Table 1.

2.2.2. Particles morphology

The prepared nanoparticles were observed by scanning electron microscopy (HITACHI SU 1510). A small amount of particles in powder form was layered on the SEM stub and then coated with gold metal using a sputter coater (Cressington 108 auto).

The mean diameter of the particles and the size distribution were analyzed by laser light diffractometry technique (SHIMADZU—SALD 7001). All measurements were carried out on suspensions of particles in acetone after sonication for 15 min at room temperature using a sonication bath (Bandelin Sonorex).

2.2.3. X-ray photoelectron spectroscopy

In the aim to characterize the chemical environments and compositions, X-ray photoelectron spectrometry (XPS) measurements were performed on a Thermo K-alpha spectrometer

with a hemispherical analyzer and a microfocussed (analysis area was c.a. 40 μm^2) monochromatized radiation (AlK α , 1486.6 eV) operating at 72 W under a residual pressure of 1×10^{-9} mbar. The pass energy was set to 20 eV for high resolution core levels spectra and 150 eV for large scale spectra. The instrument work function was calibrated to give a Binding Energy (BE) of 83.9(6) eV for the Au 4f $_{7/2}$ line for metallic gold and 932.6(7) eV BE for the Cu 2p $_{3/2}$ line of metal copper. Charge effects were compensated by the use of a charge neutralisation system (low energy electrons) which had the unique ability to provide consistent charge compensation. All the neutraliser parameters remained constant during analysis and allow ones to find a 285.0 eV C1s binding energy for hydrocarbon. Peaks convolution was processed with a nonlinear Shirley-type background (Shirley, 1972) and mathematical components were optimized with a weighted least-square fitting method using 70% Gaussian, 30% Lorentzian line shapes. Quantification was performed with CasaXPS processing software (CasaXPS Ltd., Teignmouth, UK) using Kratos Relative Sensitivity Factors's library (Scofield, 1976). Binding energies are given with a ± 0.2 eV precision. The mounting of the nanoparticles has been limited to a thin powder deposition onto a conductive copper paste for the XPS analysis. To prevent the samples from moisture/air exposure, the XPS spectrometer is directly connected to an argon dry-box working at low H $_2$ O /O $_2$ level (<1 ppm through a fast load transfer chamber).

2.2.4. Maximum swelling degree

The gravimetric method was used in order to determine the swelling degree of the nanocapsules in slightly alkaline aqueous medium (phosphate buffer solution, pH 7.4) and in the acidic medium (acetate buffer solution, pH 3.3). For this, a certain amount of dried sample (w_0) was immersed into the buffer solution and maintained under magnetic stirring at 25 °C. After 24, 48 and 72 h the nanocapsules suspension was ultracentrifuged (15,000 rpm) and the swollen sample (w_1) was weighed. The traces of water were removed by using a piece of filter paper. The swelling degree was calculated with the following equation:

$$Q(\%) = \frac{w_1 - w_0}{w_0} \times 100 \quad (1)$$

In order to diminish the errors which can interfere with the real measurements, the swelling degree was measured after 24, 48, 72 and 96 h. The results represent the arithmetic average of three different determinations, the standard deviation being lower than 10%.

2.2.5. CF loading and in vitro release

CF was used as drug for the *in vivo* and *in vitro* release tests. For loading experiments 20 mg of capsules (sample C7.9) were suspended in 1 mL CF solution (25 mg/mL) and dispersed in a sonication bath for 15 min. The suspension was maintained under stirring for 24 h and then centrifuged for 15 min at 15,000 rpm and finally freeze-dried (Laboratory freeze-dryer Christ Alpha 1–4). The CF encapsulation efficiency has been calculated by determining the CF content in the supernatant in correlation with the standard calibration curve by using UV–vis spectroscopy (Nanodrop ND 1000) at 275 nm wavelength.

Concerning the release experiments a certain amount of CF loaded particles were introduced in cellulose dialysis tubes immersed in 20 mL buffer solution at 37 °C, in a water bath, under continuous shaking. Small aliquots of buffer solution were withdrawn at appropriate time intervals and the CF concentration was determined by UV–vis spectroscopy (Nanodrop ND 1000) at 275 nm.

2.2.6. In vitro enzymatic degradation

Starting from the idea that gelatin is in fact a collagen hydrolysate, the ability of capsules to degrade on exposure to enzymes was studied by using *collagenase* which represents the main enzyme responsible for *in vivo* degradation of native collagen fibrils in different eye diseases such as Keratomalacia (rapid corneal ulceration that occurs in children who are severely deficient in vitamin A) (Seng et al., 1980), corneal destruction after injury and alkali-induced burns. (Elner et al., 2003a) or associated with other diseases (Riley et al., 1995).

The process was evaluated by measuring the amount of α -NH₂ groups (mmol/mL $\times 10^{-10}$) after enzyme action, by means of ninydrin test.

Briefly, the ninydrin reagent was prepared by dissolution of SnCl₂·2H₂O (0.032 M) in citrate buffer solution pH 5.0, (500 mL), and the addition of 500 mL solution of ninydrin (20 g) in 2-methoxyethanol.

The initial samples were incubated in 30 mL PBS (0.01 M) pH 7.2, containing 0.01% collagenase in a shaking water bath at 37 °C. At preestablished time intervals, 1 mL of sample solution was withdrawn, mixed with ninydrin reagent (5 mL) and quenched in boiling water for 20 min, followed by a rapid cooling (within 5 min; ice bath) to room temperature. Then, water/2-propanol solution (1:1, v:v), (25 mL) was added and optical absorbance was recorded (570 nm using a UV–vis spectrophotometer–BOECO S 30).

The degradation degree was calculated from the calibration curve of gelatin degradation and the equations:

$$DD = \frac{C_n}{C_0} \times 100, \quad (2)$$

where DD is the degradation degree (%), C_n the nanocapsule concentration in primary amino groups (mmol NH₂/mL), C₀ the maximal concentration in primary amino groups from gelatin (mmol NH₂/mL) and

$$DE = \frac{C_n}{C_{nmax}} \times 100 \quad (3)$$

where DE is the degradation efficiency (%) and C_{nmax} the maximal concentration in primary amino groups of nanocapsules (mmol NH₂/mL).

2.2.7. In vivo ocular biodistribution

For preparing fluorescent labelled capsules the chitosan has been labelled with fluorescein by following the method of De Campos et al. (2004). Fluorescein was covalently attached to chitosan: the reaction has been taken place between the amine groups of chitosan and carboxyl groups of fluorescein (Fig. 1), the amidation reaction being catalysed by EDAC.

Briefly, a certain amount of CS was dissolved in 1% acetic acid solution to obtain a final concentration of 1%. The amounts of fluorescein and EDAC have been calculated in order to have half of the chitosan free amine groups to react with fluorescein, the rest being necessary later for reaction with TPP and GA, respectively, the pH of the solution has been adjusted to 6 with NaOH (1 M). The demineralised water has been added in order to have a final solution volume of 250 mL. Separately, the specific amount of fluorescein has been dissolved in ethanol in order to have 10 mL with a concentration of 10 mg/mL. These two solutions were mixed together and the specific amount of EDAC has been added in a final concentration of 0.05 M. The mixture was allowed to react in the dark for 24 h at room temperature. The conjugate was purified by dialysis (cellulose dialysis tubing, pore size 12,400 Da) against demineralized water, 0.05 N NaOH solution, and finally against de-mineralized water and then lyophilized. With this derivatized chitosan, particles have been obtained following the procedure presented above.

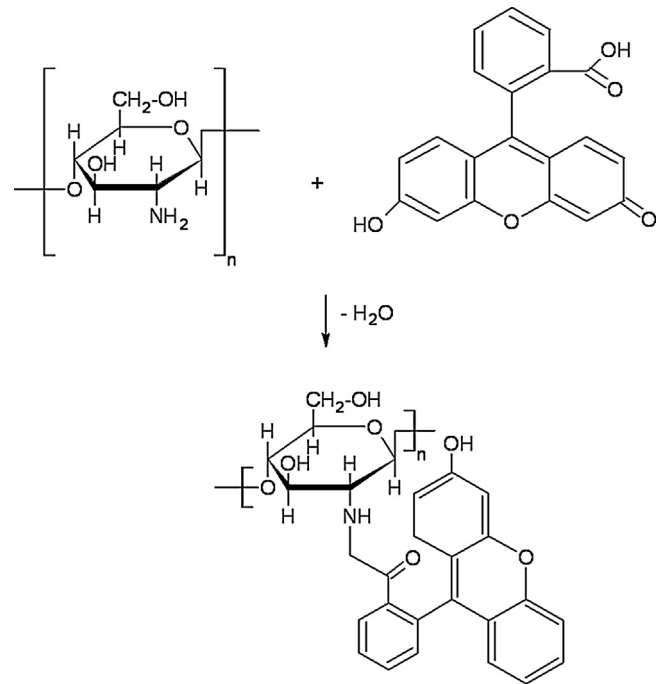


Fig. 1. Chitosan–fluorescein reaction.

For *in vivo* ocular biodistribution test, one series of 9 Wistar rats have been used, weighing 150–180 g. The left eye was used as control: it has not received any treatment and the fluorescent nanoparticles suspension (the concentration of nanoparticles in physiological serum, being equal to 1%) has been intravitreal administered in the right eye after a general anaesthesia with Ketamin (0.1 mL/100 g b.w.). The injected eyes have been enucleated and the animals euthanized at the end of the experiment. The eyes have been transferred on ice and sectioned immediately after the enucleation. All ocular tissue sections have been treated with monoclonal anti-fluorescein antibodies (produced in mouse–FL-D6 clone–Sigma–Aldrich) using a dilution of 1/400 at room temperature. After 48 h, the primary antibodies have been removed by successive washings with PBS and the samples were treated with anti-mouse secondary antibodies (the whole molecule of IgG; produced in goat and labelled with R-phycoerythrin–Sigma–Aldrich) for 1 h at a dilution of 1/100 and room temperature.

All sections have been transferred on microscope slides and covered with specific medium for fluorescence (0.1% DABCO in PBS; glycerol for microscopy 1:1). For fluorescence analysis a Nikon Eclipse TE300 Inverted Microscope has been used (40 \times). The excitation wavelength was setup at 514 nm and for emission a filter having 570 nm wavelength has been used for R-phycoerythrin. The images have been captured using the software associated to the microscope in two modes: red fluorescence for R-phycoerythrin and transmitted light for morphological structures of the samples. The final processing has been performed using the software Image J (NIH) for the superposition of the two types of images and measurement of red intensities (arbitrary units). The red fluorescence intensities were calculated starting from RGB diagrams.

2.2.8. In vivo cefuroxim release study

The *in vivo* tests were performed on Wistar rats having each a weight of 300 g. Each subject was sedated by intraperitoneal injection of a Thiopental solution, 5 mg/kg body weight. When the anesthesia was effective the drug loaded particles were injected in the left eye, 50 μ L of 1% particles suspension containing an

estimated drug quantity of 4×10^{-4} g. The same amount of drug was injected also in the right eye but as free cefuroxim in a 20 μ L solution. Both eyes of each animal were eviscerated under anesthesia at fixed time intervals, 15 min, 30 min, 1 h, 2, 3, 4, 5, 6, 24, 48 and 92 h, respectively. At specific time points (during 5 h) the same amount of vitreous was extracted and analyzed by HPLC-MS technique (the rats were euthanized at the end of the extraction). The samples were suspended in 2 mL water/acetonitrile mixture 1/2 using an Ultraturrax at 5000 rpm. The obtained eye homogenate was centrifuged at 11,000 rpm and 0.5 mL of the supernatant was filtered through 200 μ m PTFE filters and further used for quantitative measurements by LC MS (10 μ L per injection).

For the LC-MS analyses of cefuroxim a standard quantitative curve was established using eye homogenate without any addition of cefuroxim. The analyzed samples were obtained by spiking clean homogenate extract, obtained as previously described, with fixed amounts of cefuroxim (CF) stock solution, thus resulting solutions of 0.2, 0.8, 1, 1.6, 5, 10, 20 μ g/mL, respectively. This resulted in a standard curve used for quantitative measurements. The solutions were stored at 4 °C avoiding light for using.

2.3. Sample extraction procedures

The samples were suspended in 2 mL water/acetonitrile mixture 1/2 using an Ultraturrax at 5000 rpm for 1 min. The obtained eye homogenate was centrifuged at 11,000 rpm and 0.5 mL of the supernatant was filtered through 200 μ m PTFE filters and further used for quantitative measurements by LC MS (10 μ L per injection).

2.4. Method validation

To evaluate selectivity, drug-free eye homogenate samples from 6 individuals were analyzed to check for the presence of any interfering peaks at the elution times of cefuroxim. The calibration curves were constructed using 7 standards ranging in concentration from 0.2 to 20 μ g/mL. The validity of the linear regression equation was indicated by the correlation coefficient ($R^2 = 0.995$).

The intraday and interday precision and accuracy were evaluated by assessing QC samples at the following concentrations: LLOQ (0.1 μ g/mL), low (0.2 μ g/mL), medium (1.6 μ g/mL), and high (20 μ g/mL).

The extraction recovery and matrix effect of cefuroxim for three concentrations of QC samples was determined by comparing the

response of CF spiked eye homogenate after extraction to that of analyte spiked into the solution extracted from blank eye homogenate and the response of CF spiked after extraction to that of CF dissolved in mobile phase, respectively.

Stability experiments were performed by leaving the eye homogenate sample at room temperature for 6 h (no light), placing the treated eye homogenate in an autosampler for 24 h and storing for 100 days at -20 °C, using three similar samples of each QC sample with three different concentrations.

2.5. Mass spectrometry measurements

The mass spectrometry setup for the quantitative measurements consists in an Agilent 6510 Triple Quad LC MS system (Agilent, USA) controlled using the MassHunter software. The CF samples were analyzed by MRM. CF fragmentation (Fig. 2) in negative mode was found to be the most sensitive in the given MS conditions and was used for further quantitation.

The chromatographic conditions for the CF separation were as follows: isocratic solvent flow 1 mL/min, constant temperature of 30 °C, mobile phase—acetonitrile/water 7/3 spiked with 1 mM HCOOH and Agilent ZORBAX 300SB-C18 4.6 \times 150 mm, 5 μ m C18 column. ESI source parameters were established for the best sensitivity: Vcap = 4000 V, fragmentor voltage = 200 V, drying gas temperature = 325 °C, drying gas flow = 12 L/min, spraying pressure = 35 psi g. The gas used by ESI source is nitrogen provided by an external source, Peak Scientific. The CF fragmentation performed in the collision cell were obtained at $E_{lab} = 5$ eV using high purity nitrogen as collision gas. The monitored fragmentation reaction characteristic for CF (Fig. 3) was m/z 423 \rightarrow (m/z 207 + 318 + 362). The LC-MS/MS conditions were established for best sensitivity by elimination as much as possible the matrix effects. LC-MS/MS peak present at retention time 1.85 min (Fig. 3A) was integrated and further used for quantitation (quantitation curve $y = 6E + 09x + 1328.9$). Thus, the LC-MS experiment was divided in three segments (see also Fig. 3B):

- first segment—the flow is directed to ESI source (0–0.9 min).
- second segment—the flow is diverted to waste in order to avoid the matrix effects over the ESI measurements (0.9–1.5 min).
- third segment—the flow is directed to ESI source and the MRM of CF is performed (only MS/MS spectra of 423 peak are quantified at 1.85 min) (1.5–2.4).

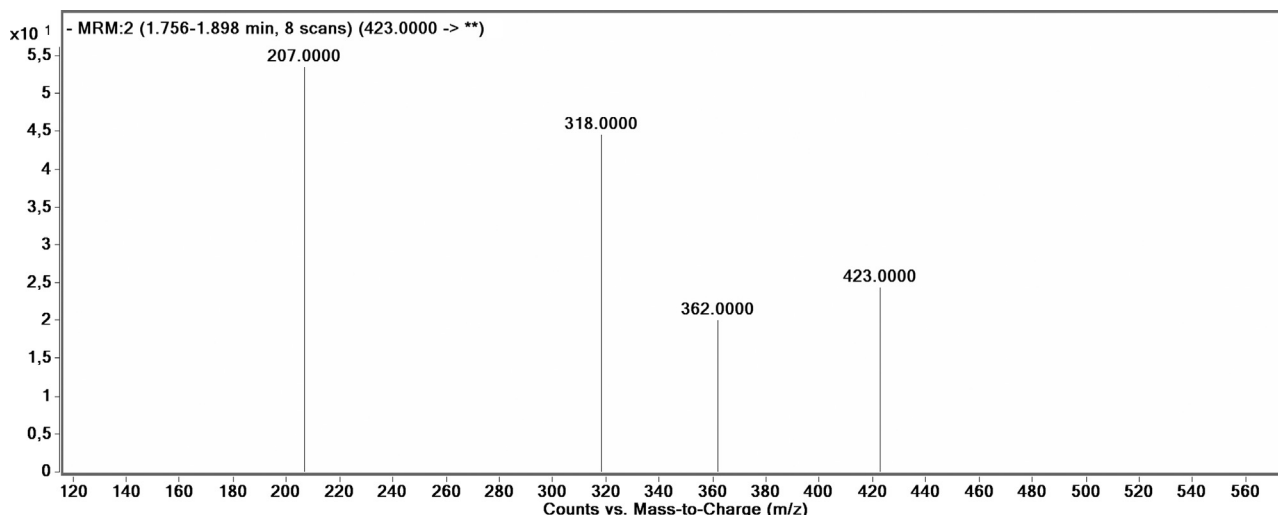


Fig. 2. ESI MS/MS of cefuroxim.

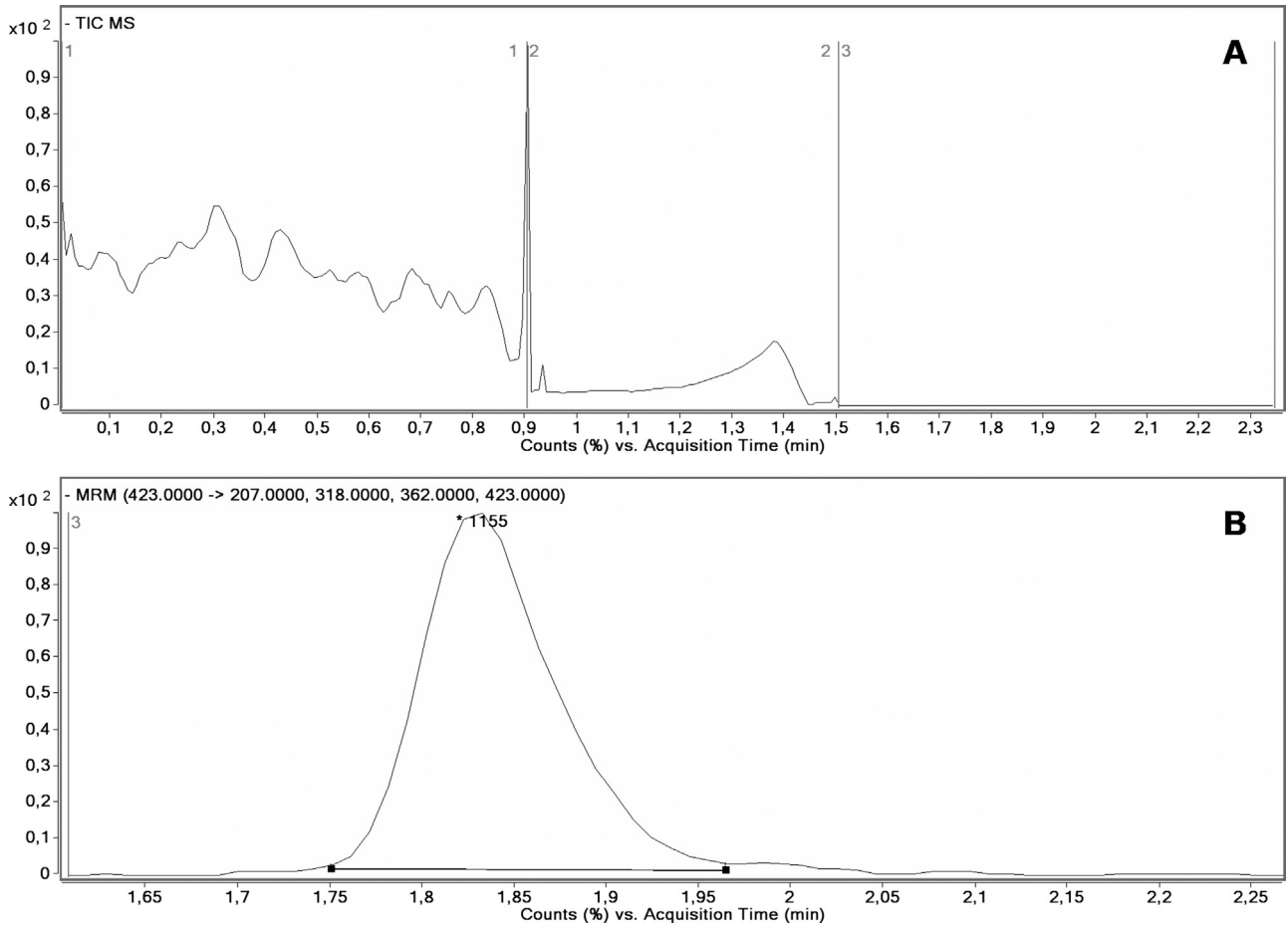


Fig. 3. LC MS chromatograms (A) total ion chromatogram; (B) MRM chromatogram for CF detection.

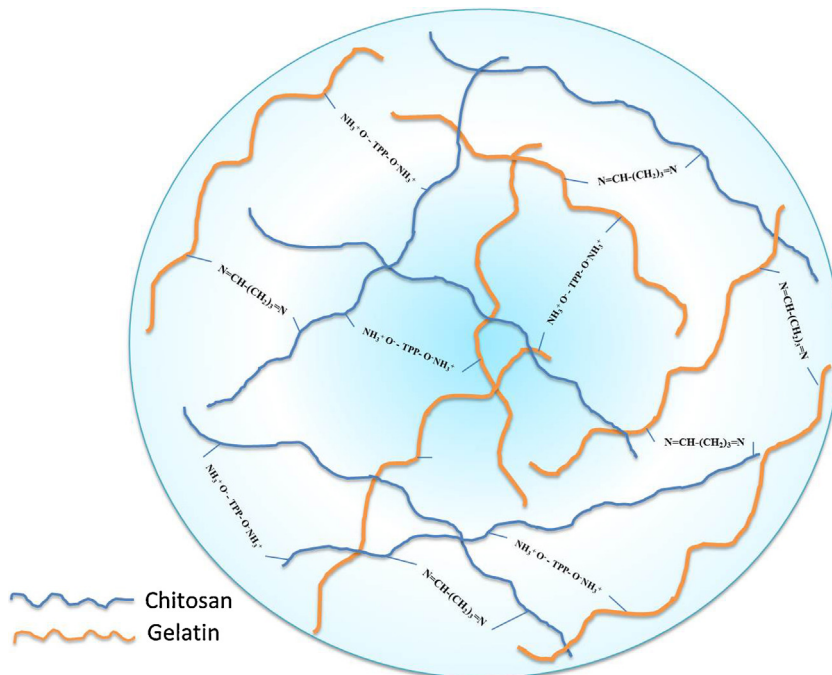


Fig. 4. Double crosslinking mechanism.

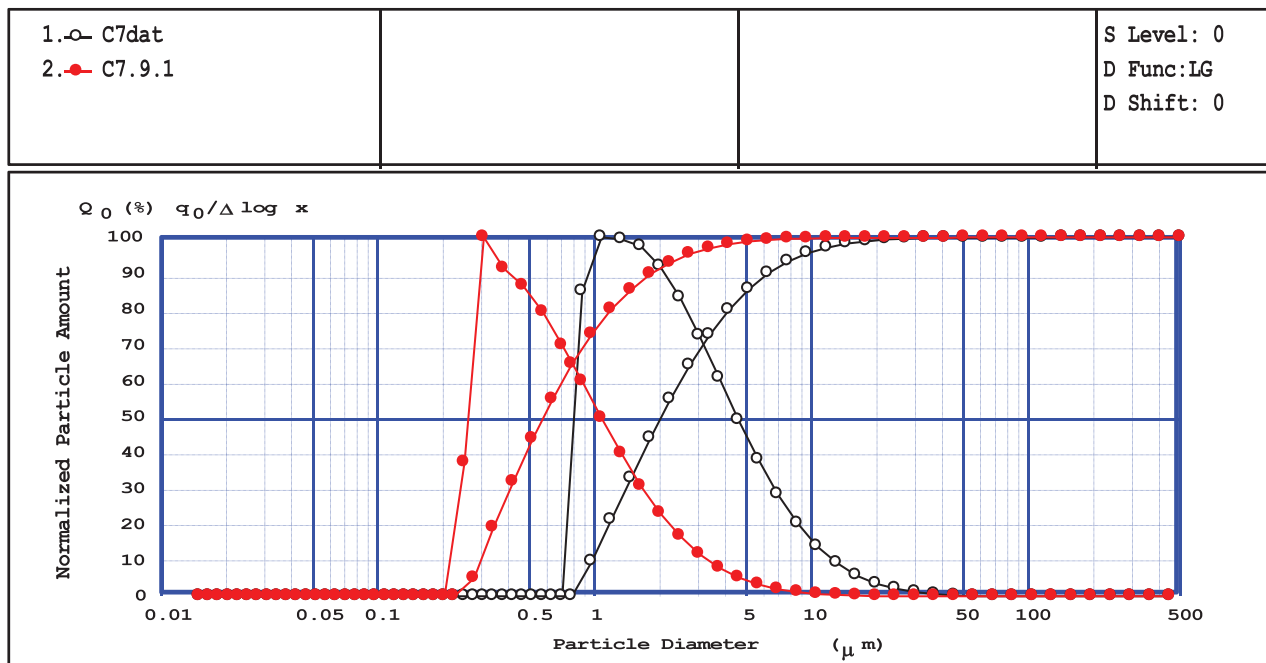


Fig. 5. Dimensional distribution of the samples C7 and C7.9.

3. Results and discussions

The capsules preparation process is an original one derived from another method previously developed in our group (Peptu et al., 2010) starting from the point that we wanted to prepare superior particles in terms of morphology and encapsulation efficiency. The double crosslinking was performed in order to maintain the stability of the polymer particles (which is generally given by the crosslinker bridges between the two types of macromolecules) without the increase of the toxicity of the particulate system. In this case that means the use of a minimal amount of the covalent crosslinker (GA) enough to stabilize the already formed gel particles (obtained after the ionic bonding of the polymers with TPP). The crosslinking mechanism is presented graphically in the Fig. 4.

One of the major advantages of the present method is represented by two natural polymers used both presenting excellent properties which make them suitable for many kinds of biomedical applications. In addition, in this case, we have tried to ensure a very good stability of the particles by using chitosan which will form the majority of the chemical bonds (both ionic and covalent) because it presents a higher number of free amine groups

(susceptible for ionic/covalent crosslinking) in comparison with gelatin which present a very small amount of free amount groups but which will ensure the formation of the interpenetrated network. Moreover, the addition of gelatin will ensure the high swelling capacity of the particles which will determine the high drug encapsulation efficiency (see the following sections).

3.1. Morphological analysis (size and shape)

The morphology represents the main characteristic which has been considered for the capsules optimization process. For this, the first studied parameters of the double crosslinking process were the TPP concentration (samples C1–C4) and the molar ratio between polymers (free amine groups) and the ionic crosslinking agent (TPP) (samples C5–C7). After these two steps an optimal sample from the morphological point of view has been selected (C7). The following steps were represented by the samples obtained after the variation of the ionic crosslinking time (C7.1–C7.3), the molar ratio between polymers (free amine groups) and the covalent crosslinking agent, GA (C7.4, C7.5), the stirring speed (C7.6) and the surfactant amount (C7.7, C7.8). The optimal sample C7.9 has been obtained by using for the preparation of the particles

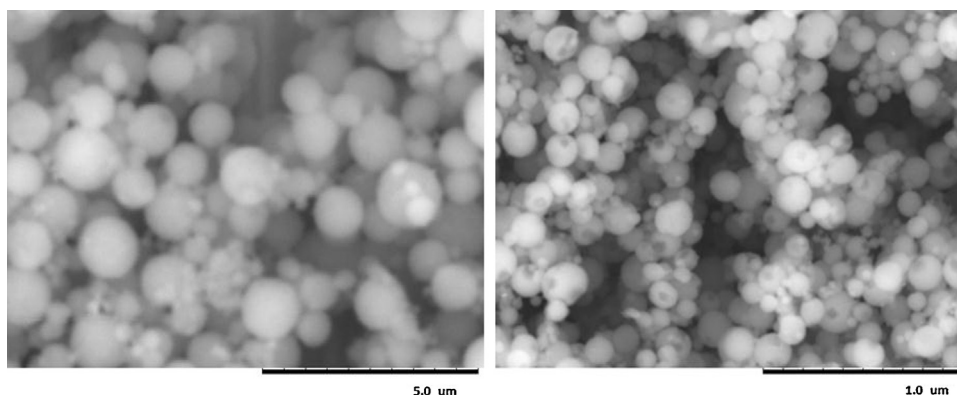


Fig. 6. Scanning electron microscopy images for the optimum samples C7 and C7.9.

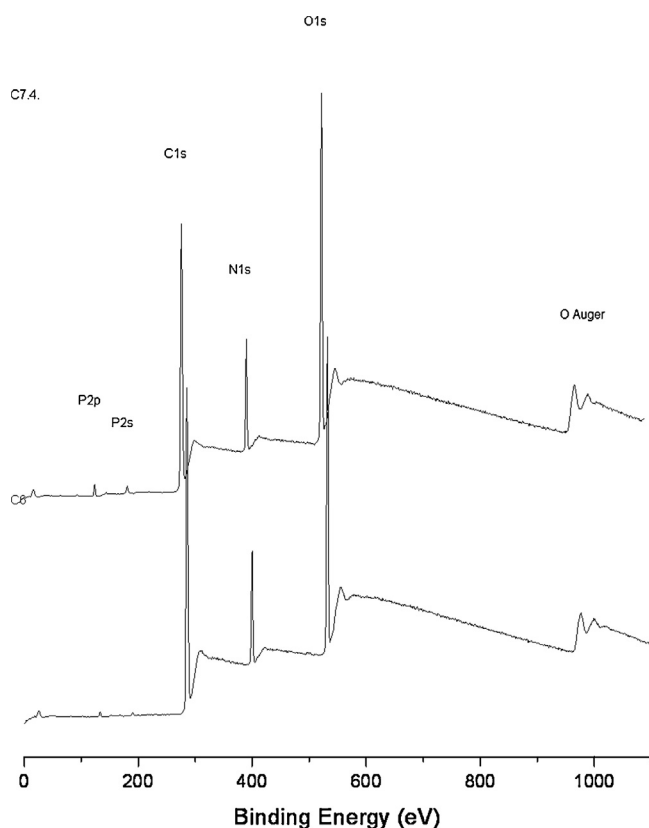


Fig. 7. Large scale spectra of samples with different ratios between ionic (TPP) and covalent (GA) crosslinking agents (C7.4 and C6).

the optimal values of the previously described parameters. In the end we have tried to see if changing the initial polymer ratio (C7.9.1–C7.9.3) allows obtaining a better morphology.

In the Table 1 the mean diameter for each sample has been presented. The sample C7 followed by the optimum sample C7.9 have been chosen taking into account both size and spherical shape characteristics as well as the aggregation tendency which can further cause problems during the *in vivo* tests. The dimensional distribution of the optimum samples C7, respectively C7.9 is represented in the Fig. 5.

SEM images of the first samples (C1–C4) indicated the formation of aggregates and a relative high polydispersity, but they present a good dispersability in water and organic solvents after stirring or ultrasonication. Dimensional polydispersity is high and aggregates are observed for the samples with different

polymer ratios (C7.1–C7.3). After the first optimization steps, the particles are better individualized (probably due to the increasing of the ionic crosslinking time or the amount of the covalent crosslinker (C7.4, C7.5) allowing the maturation of the particles). By changing the initial amount of the surfactant and the stirring speed, particles with nanometric size with a clear round shape and without aggregates have been obtained. In the Fig. 6 SEM photographs for the most representative samples are presented.

3.2. X-ray photoelectron spectroscopy

In Fig. 7, spectra of samples with different ratios between ionic (TPP) and covalent (GA) crosslinking agents (samples C7.4. and C6) were recorded in a large energy scale (0 eV–1100 eV). P_{2p} peaks are observed confirming the ionic crosslinking and the signal is lower for GA/TPP=0.83 as expected. For high energy resolution, the spectra are better resolved and mathematical convolutions give access to the different chemical functions in the composites. Samples were compared considering the difference in the content of specific crosslinking agents. Specific C_{1s} , P_{2p} , N_{1s} and O_{1s} regions were then examined and results are reported in Table 2.

Concerning the nitrogen species detected, the N_{1s} spectra (Fig. 8) exhibit three components which were assigned to: N–C bonds (Wagner et al., 2003) at 400.0 eV, amino groups in the ammonium form (Amaral et al., 2005) at 401.9 eV. The supplementary peak at 398.6 eV is the signature of the covalent crosslinking (N=C, (Beamson and Briggs, 1992) with glutaric aldehyde as given in the scheme.

For phosphorus entities present in the composites, all spectra revealed a doublet ($2p_{3/2-1/2}$ components at respectively *c.a.* 133.5 eV and 134.4 eV) clearly associated with HPO_4^- chemical groups (Wagner et al., 1979) operating in the ionic crosslinking. Moreover the O_{1s} peak at 533.9 eV corresponds to same HPO_4^- units (Quan et al., 1989) confirming the ionic crosslinking.

Comparing the relative abundances (atomic percentages) of elements, a correlation exists between the ratio of specific peaks and the ratio between covalent and ionic crosslinking agents. As examples, the relative abundance of the peak assigned to N=C groups (N_{1s} spectrum) is higher for the sample with an important covalent crosslinking agent content (sample a), whereas highest intensities of O_{1s} peak at 533.9 eV and N_{1s} peak at 401.9 eV (interactions between HPO_4^- and NH_3^+) were observed for sample b with a high content of ionic crosslinking agent. In the same time the relative abundances of each of the elements are in good agreement with the ratio between the different crosslinking agents (Table 3)

Calculating the ratio amine groups ionically bonded/amine groups covalently bonded, close to 1 (Table 4, line 8), results that,

Table 2

Peak positions and relative abundance (atomic percentages) for Samples a (GA/TPP=0.042—sample C7.4) and b (GA/TPP=0.83—sample C6).

Peak	GA/TPP=0.042 (Sample a)			GA/TPP=0.83 (Sample b)		
	Position (eV)	FWHM (eV)	at.%	Position (eV)	FWHM (eV)	at.%
C 1s	285.0	1.5	28.1	285.0	1.4	43.4
	286.3	1.4	21.2	286.4	1.4	19.1
	287.9	1.5	12.3	287.9	1.3	8.8
	288.9	1.5	3.2	288.9	1.3	2.4
N 1s	398.6	1.4	0.4	398.6	1.5	0.6
	400.0	1.6	8.5	400.0	1.6	8.1
	401.8	1.6	1.4	402.0	1.7	0.7
	531.5	1.8	10.6	531.6	1.9	8.8
O 1s	532.7	1.5	9.5	532.8	1.5	6.3
	533.9	1.6	2.9	533.9	1.4	1.2
	533.9	1.6	1.3	133.4	1.5	0.4
	134.4	1.6	0.6	134.3	1.6	0.2
P 2p _{3/2-1/2}	133.5	1.6	1.3	133.4	1.5	0.4
	134.4	1.6	0.6	134.3	1.6	0.2

FHWM: full width of peaks at half maximum.

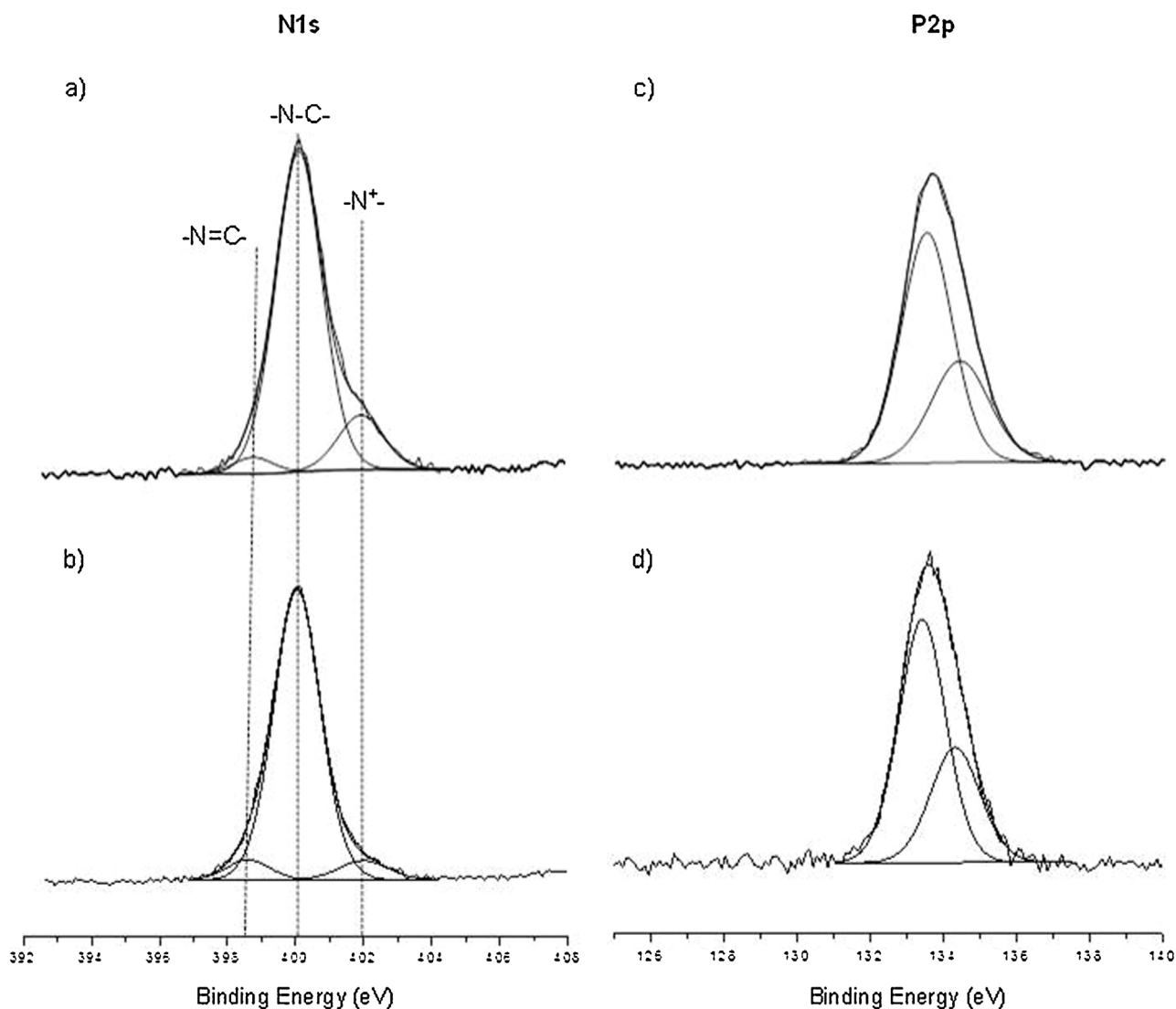


Fig. 8. XPS spectra of GA-TPP composite with: GA/TPP = 0.042 ((a) N1s peak and (c) P2p_{3/2-1/2} peak); GA/TPP = 0.042 ((b) N1s peak and (d) P2p_{3/2-1/2} peak).

on particles surface, the same number of amine groups participates to each type of crosslinking bond. The GA is added in a smaller amount compared with TPP and, as expected, the covalent crosslinking has taken place at the particle surface not in the entire volume, whereas the ionic crosslinking is taking place in the whole volume of the aqueous polymer drops.

3.3. Swelling degree

Swelling experiments lead to interesting results showing that the maximal swelling degree is in very good correlation with particles preparation parameters. In Fig. 9 a general view over these parameters is presented and the first conclusion is that for all samples, the maximal swelling degree in acetate buffer (pH 3.3) is higher (between 804 and 1587%) than in phosphate buffer (pH 7.4) (between 516 and 1121%). This effect is determined by the amine groups of the two polymers which have not participated to the crosslinking process (both ionic and covalent). In acid environment the amine groups are quaternized into ammonium groups; the electrostatic repulsions between these groups increase the distances between the network chains determining the accumulation of high amount of water. The maximal swelling degree is

high in alkaline pH too: in these conditions an important role is given to the carboxylic groups of gelatin coming from the dicarboxylic acids present in its structure. In basic media, these groups are as carboxylate anions which determine electrostatic repulsions but not as strong as those developed in acidic pH giving a high maximal swelling degree but lower than in alkaline pH. These results are in good agreement with other previous studies (Mi et al., 2003; Shu and Zhu, 2002a; Boral et al., 2006)

Analysing the C1–C4 series one can notice that increasing TPP concentration reduces the maximal swelling degree, as a logical consequence of increasing the network crosslinking density. A similar effect was noticed in the series C1, C5, C7 when increasing the amount of TPP, the maximum swelling degree is reduced.

Table 3

Relative abundance (atomic percentages) of elements within the particles with different crosslinking agents ratios (Samples C7.4 (GA/TPP = 0.042) and Sample C6 (GA/TPP = 0.83)).

	at.% C	at.% N	at.% P	at.% O
Sample C7.4	64.8	10.3	1.9	23.0
Sample C6	73.7	9.4	0.6%	16.3

Table 4

XPS quantitative aspects regarding surface structure of two types of particles.

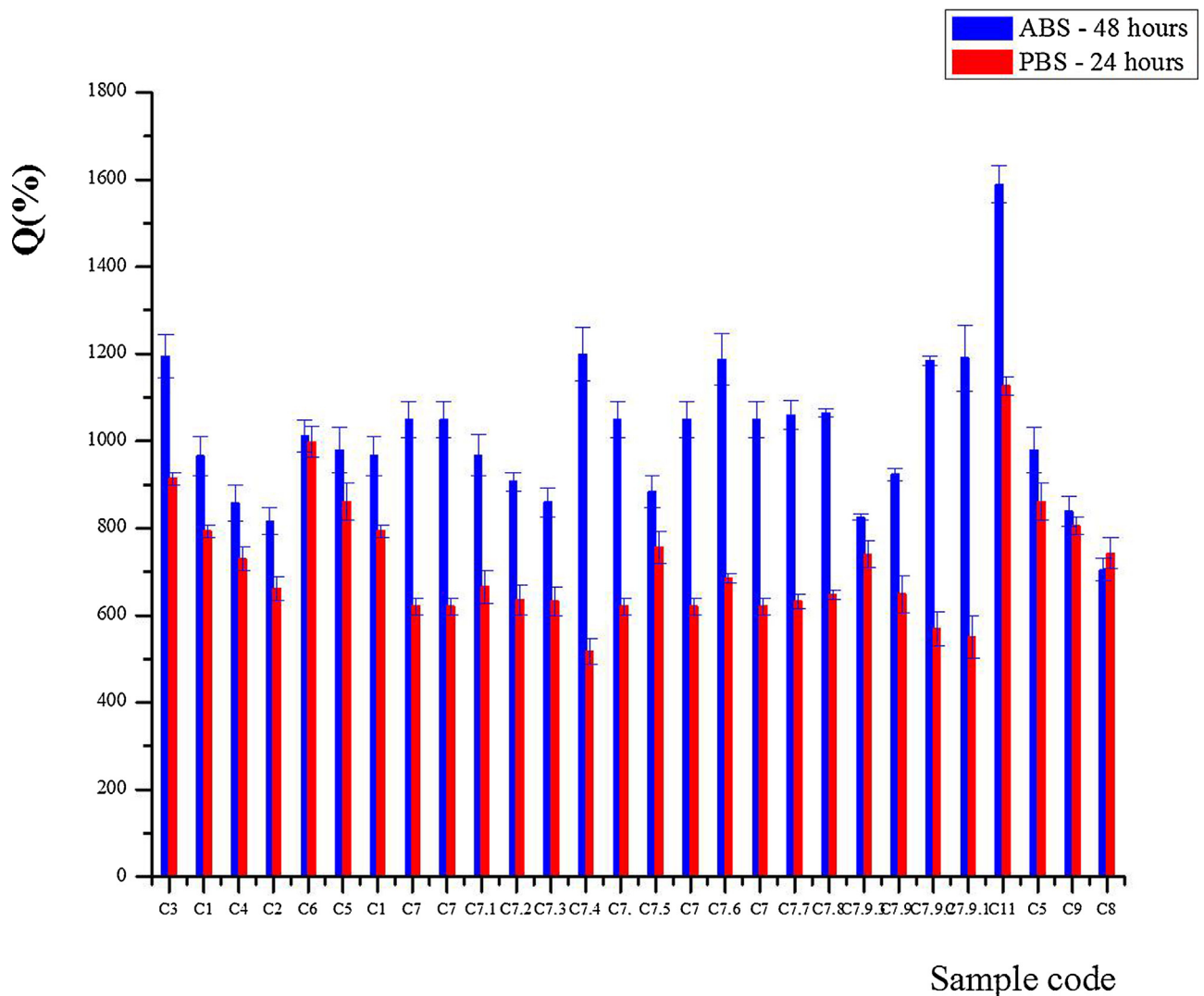
Property	Value	
	C7.4	C6
1. TPP in initial mixture, (mol)	6.2×10^{-4}	6.21×10^{-5}
2. TPP chemically bonded, on the surface (mol)	2.45×10^{-5}	2.56×10^{-5}
3. TPP bonded on the surface, (reacted mols/initial mol) $\times 100$, (%)	3.95	41.22
4. GA added initially, (mol)	11.18×10^{-5}	22.37×10^{-5}
5. GA covalently bonded (mol)	7.57×10^{-5}	7.93×10^{-5}
6. % GA chemically bonded reacted mol/total mol $\times 100$, (%)	67.71	35.44
7. Nitrogene amount participating to ionic crosslinking, (mol)	8.14×10^{-5}	8.52×10^{-5}
8. <small>Amine groups ionically bonded</small> <small>Amine groups covalently bonded</small>	$\frac{8.14 \times 10^{-5}}{7.57 \times 10^{-5}} \times 1.075$	$\frac{8.52 \times 10^{-5}}{7.93 \times 10^{-5}} \times 1.074$

Other researchers have obtained similar results (Shu and Zhu, 2002b).

The C7–C7.4 samples are different by the ionic crosslinking time from 1 h to 4 h. As it was predictable, increasing the ionic crosslinking time will determine obtaining denser networks with lower maximal swelling degree values in total agreement with other researches (Ko et al., 2002). Following the same reasoning in the series C7.4, C7.8, C7.5 when an increasingly higher amount of GA was used the maximal swelling degree was lower as observed in other similar studies (Silva et al., 2004). Stirring speed (used for

emulsion preparation) and the amount of surfactant does not present an influence on the swelling degree, since these parameters do not interfere in the chemistry of the crosslinking process.

The composition of initial polymer mixture represents an important parameter for swelling degree evaluation. Reducing CS amount from 100% (C8) to 25% (C11) leads to higher swelling degree, the phenomenon having a simple explanation: reducing the amount of CS means a reduced number of amine groups participating to both types of crosslinking sites, then the

**Fig. 9.** Swelling degree (SD) in different pH conditions.

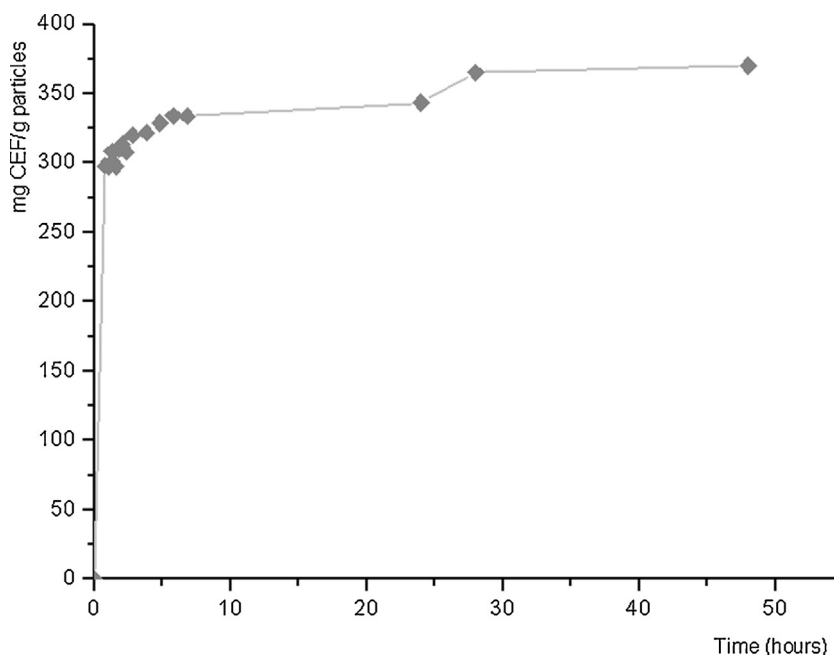


Fig. 10. CF release kinetic in pH 7.4 environment.

crosslinking density is also reduced which makes the swelling degree to be higher. In addition, G presents a superior hydrophilicity determining the accumulation of higher amount of water.

3.4. In vitro drug release

For loading and release studies sample C7.9 was considered optimal. For this sample a toxicity test has been performed using the determination of average lethal dose (DL50) according to a method which was previously described in one of our published paper (Peptu et al., 2010). In conformity with Lodge and Sterner scale (Danila, 1984) the tested nanoparticles are in the category of “practically nontoxic”.

The cefuroxime encapsulation efficiency for tested sample was around 47%. The dried sample was then tested for *in vitro* release characteristics. The release kinetics in alkaline environment (pH

7.4) is presented in Fig. 10. The release behavior is typical of diffusional systems like this one. A relative strong burst effect has been noticed in the first hour, afterwards the system is equilibrating and slowly release CF for 48 h tested.

3.5. In vitro enzymatic degradation

The particles composition includes two natural polymers known as being degradable under the effect of specific enzymes. CS is degraded by chitosanase by endohydrolysis of beta-(1 → 4)-linkages between D-glucosamine residues to monosaccharide level G, which is resulted from collagen by a controlled hydrolysis, is sensitive to collagenase which is catalyzing the hydrolysis of peptide bond in the main chain determining the appearance of ending alpha amine groups. The latter can be identified by a color reaction with ninhydrin; depending on the color intensity

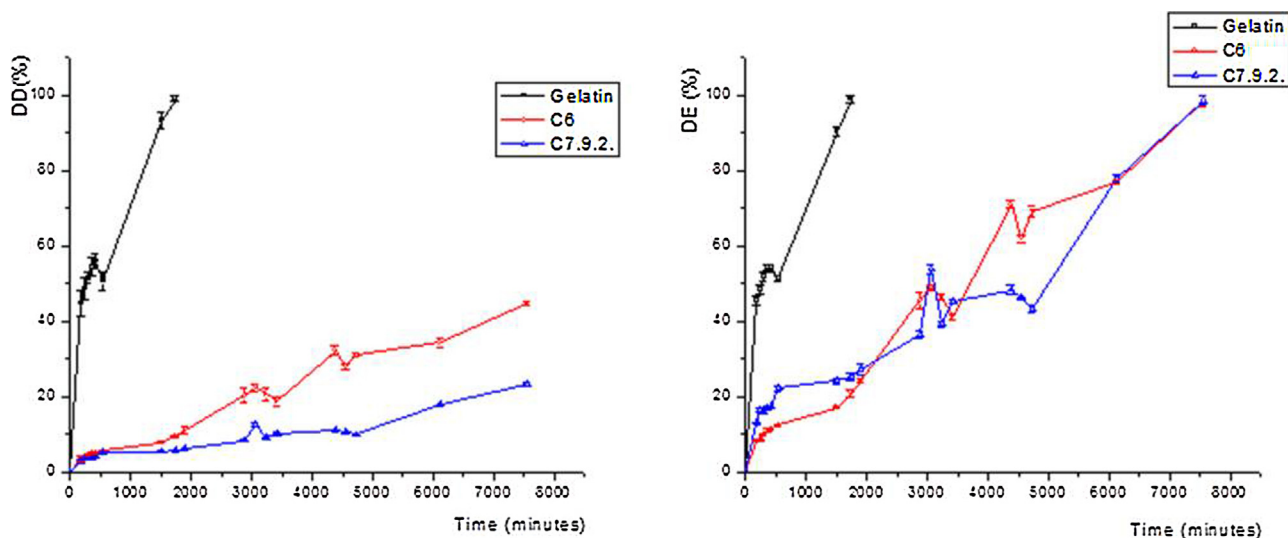


Fig. 11. (A) The variation in time of degradation degree (DD) for samples with different gelatin amount in composition (C6–50% Gelatin and C7.9.2–25% gelatin) in comparison with pure gelatin; (B) the efficiency of enzymatic degradation process (DE) as a function of time for particles with different gelatin composition (C6–50% Gelatin and C7.9.2–25% gelatin) in comparison with pure gelatin.

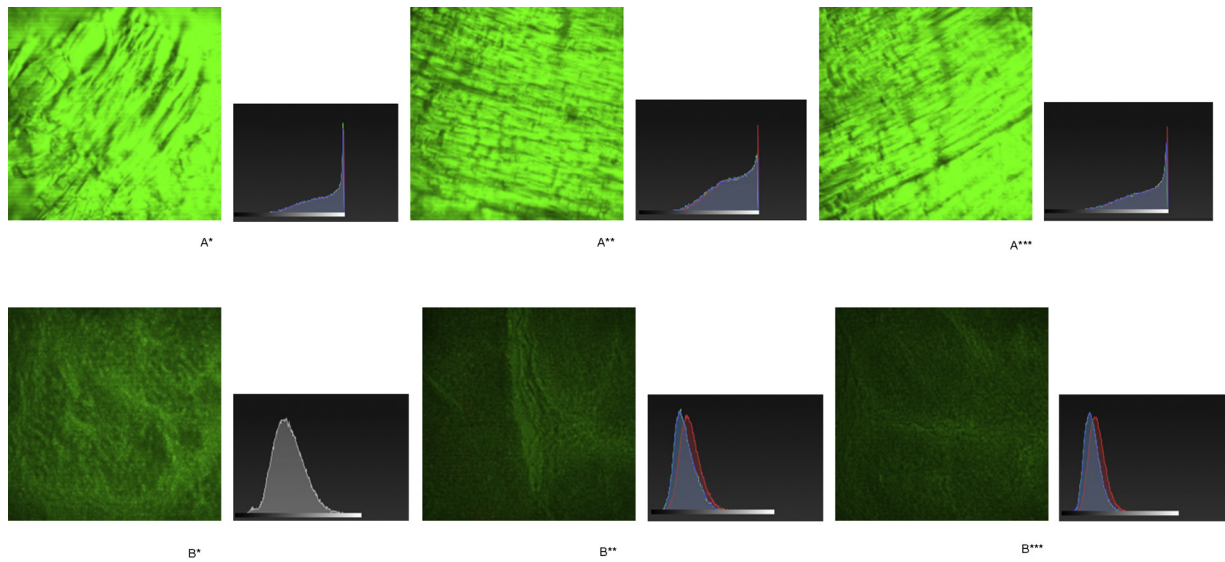


Fig. 12. Analysis of red fluorescence intensity (RGB diagram on morphology) from lens (A) and retina (B) sections, 24 h (**) and 72 h (***) as compared to the control group (*).

(spectrophotometrically determined) it is possible to analyze the degradation degree of the particles and the gelatin degradation efficiency. Collagenase has been associated with the phenomenon of cornea destruction following accidents or alkaline burns (Elnor et al., 2003b). In our experiment, the gelatin degradation efficiency (blank sample) is maximal (100%) after 29 h (Fig. 11), when the maximum alpha amine end group concentration is achieved. Gelatin from capsules is achieved after longer periods of time (126 h), this effect being due to the fact that gelatin being trapped within the interconnected network, the access of the enzyme to the amide bond is decreased. By analyzing the results presented in the Fig. 10, one can observe that after this time interval, the particles degradation degree is different depending on their composition. The degradation process presents a linear evolution,

the particles are 47% degraded for sample C6 and 25% for sample C7.9.2. These values of degradation degree are identical with the amount of gelatin in initial composition, indicating that under the action of collagenase only the protein is degrading.

3.6. In vivo ocular biodistribution

Analyzing the results of particles eye biodistribution after intravitreal administration, one can observe that the particles can reach in large quantities the lens and retina 24 h after administration (Fig. 12). This is based on the fluorescence intensity peak and surface of the fluorescence diagram analysis which allows only the qualitative estimation of the particles concentration which penetrated a certain segment of the eye. Smaller amounts (fluorescence

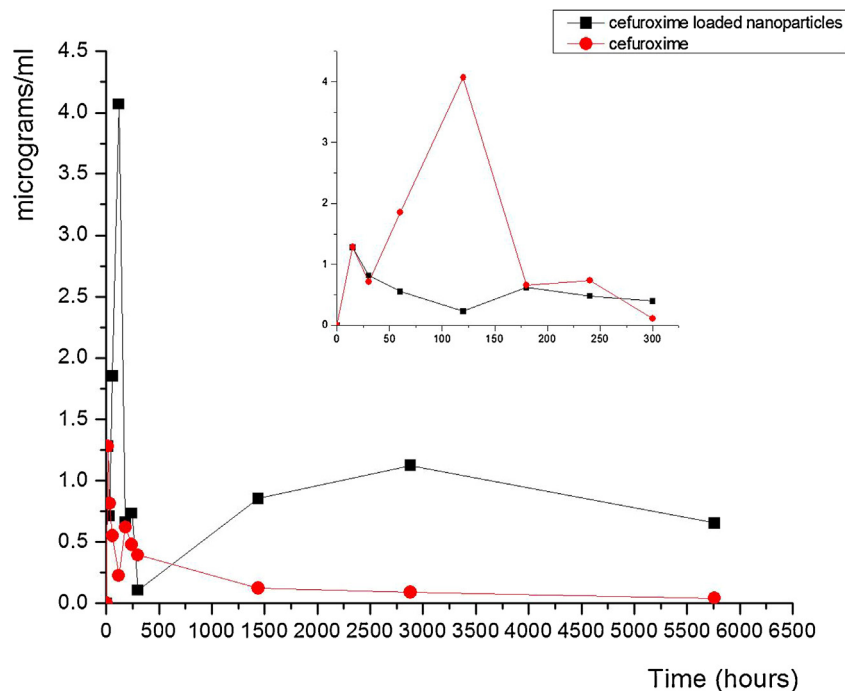


Fig. 13. In vivo cefuroxime release profile kinetic for free (red line) and encapsulated (black line) cefuroxime. (For interpretation of the references to colour in this figure legend, the reader is referred to the web version of this article.)

reduced intensity) were found at cornea and lens level also 24 h after administration (personal observation, data not shown). Although the intensity of fluorescence is lower, at 72 h the particles are still present at retinal, lens, scleral and corneal level. Thus, analyzing the biodistribution of particles it has been demonstrated their potential to penetrate the adjacent tissues of the administration site and also the deep migration to cornea and retina after longer time.

3.7. In vivo cefuroxime release behavior

The evolution in time of the CF accumulated at the level of the eye is presented in Fig. 13.

The CF was administrated as free drug solution or as CF loaded nanoparticles. The free drug administration leads to a burst effect in the first 15 min followed by relatively constant CF concentration for about 5 h. When CF is administered as nanoparticles a different kinetics is displayed. In the first 15 min the drug may be found at similar levels as in the case of free CF administration but in the interval between 50 and 200 min a sustained release may be observed. As it may be observed the difference in terms of maximal concentration of the released CF between the two administration pathways is 8 times bigger in favor of nanoparticles. This fact can be explained by a fast clearance of the drug when administered as free CF, possibly occurring during the first 15 min after administration. The nanoparticles continue to release CF even after the initial burst release up to 96 h.

4. Conclusions

Various efforts have been made by the scientific community to improve the bioavailability and the drug release rate from formulations. We consider the present results as an important step in achieving an appropriate polymer particulated system for cefuroxime release at intraocular level. The dimensions and the physical–chemical properties of the particles can be modulated (by varying the preparation parameters) to facilitate the administration, the biodistribution and the drug release in the specific segment of the eye. Therefore, the optimum reaction conditions considered for preparing nanoparticles appropriate for intravitreal administration are the following: CS/G ratio equal to 1.5% TPP concentration, $\text{NH}_3^+/\text{TPP} = 1.175$ (molar ratio), $\text{NH}_3^+/\text{GA} = 7/1$ (molar ratio), the crosslinking time—4 h, stirring speed—9000 rpm and 4% surfactant (in respect with each phase volume). This experimental study demonstrated also the ability of fluorescent nanoparticles to penetrate ocular tissues close to the administration site (intravitreal injection) and especially their tendency to migrate deep in the retina at time intervals of 72 h.

To conclude, although further experiments are warranted, all these results point out CS–G particles as potentially useful candidates for drug delivery at intraocular level.

Acknowledgement

This work has been performed in the frame of the Partnership Program in priority areas—PN II, under MEN—UEFISCDI authority, project code PN-II-PT-PCCA-2013-4-1570 (project number 218/2014).

References

Alarcón, R., Martínez, M., 2006. Intraocular drug delivery systems. *Arch. Soc. Esp. Ophthalmol.* 81, 6–57.
 Amaral, F., Granja, P.L., Barbosa, M.A., 2005. Chemical modification of chitosan by phosphorylation: an XPS, FT-IR and SEM study. *J. Biomater. Sci. Polym. Edn* 16, 1575–1593.

Apaolaza, P.S., Delgado, D., Del Pozo-Rodríguez, A., Gascón, A.R., Ángeles Solinís, M., 2014. A novel gene therapy vector based on hyaluronic acid and solid lipid nanoparticles for ocular diseases. *Int. J. Pharm.* 465 (1–2), 413–426.
 High Resolution XPS of Organic Polymers. In: Beamson, G., Briggs, D. (Eds.), John Wiley & Sons, NYC, USA.
 Boral, S., Gupta, A.N., Bohidar, H.B., 2006. Swelling and de-swelling kinetics of gelatin hydrogels in ethanol–water marginal solvent. *Int. J. Biol. Macromol.* 39, 240–249.
 Cadinoiu, A.N., Popa, M., Curteanu, S., Peptu, C.A., 2011. Covalent and ionic co-cross-linking—an original way to prepare chitosan–gelatin hydrogels for biomedical applications. *J. Biomed. Mater. Res. A* 98 (3), 342–350.
 Danila, G., 1984. *Ghid de Date Toxicologice*. Editura Medicala, Bucuresti.
 De Campos, A.M., Diebold, Y., Carvalho, E.L.S., Sánchez, A., Alonso, M.J., 2004. Chitosan nanoparticles as new ocular drug delivery systems: in vitro stability, in vivo fate, and cellular toxicity. *Pharm. Res* 21 (5), 803–810.
 Delyfer, M.N., Rougier, M.B., Leoni, S., Zhang, Q., Dalbon, F., Colin, J., Korobelnik, J.F., 2011. Ocular toxicity after intracameral injection of very high doses of cefuroxime during cataract surgery. *J. Cataract Refract. Surg.* 37 (2), 271–278.
 Elner, S.G., Elner, V.M., Kindzelskii, A.L., Horino, K., Davis, H.R., Todd III, R.F., Glagov, S., Petty, H.R., 2003a. Human RPE cell lysis of extracellular matrix: functional urokinase plasminogen activator receptor (uPAR), collagenase and elastase. *Exp. Eye Res.* 76 (5), 585–595.
 Elner, S.G., Elner, V.M., Kindzelskii, A.L., Horino, K., Davis, H.R., Todd III, R.F., Glagov, S., Petty, H.R., 2003b. Human RPE cell lysis of extracellular matrix: functional urokinase plasminogen activator receptor (uPAR), collagenase and elastase. *Exp. Eye Res.* 76 (5), 585–595.
 Elzoghby, A.O., 2013. Gelatin-based nanoparticles as drug and gene delivery systems: reviewing three decades of research. *J. Control. Release* 172 (3), 1075–1091.
 Gagandeep, T.G., Malik, B., Rath, G., Goyal, A.K., 2014. Development and characterization of nano-fiber patch for the treatment of glaucoma. *Eur. J. Pharm. Sci.* 53, 10–16.
 Goswami, S., Bajpai, J., Bajpai, A.K., 2010. Designing gelatin nanocarriers as a swellable system for controlled release of insulin: an in-vitro kinetic study. *J. Macromol. Sci. A Pure Appl. Chem.* 47, 119–130.
 Hornof, M., Weyenberg, W., Ludwig, A., Bernkop-Schnürch, A., 2003. Mucoadhesive ocular insert based on thiolated poly(acrylic acid): development and in vivo evaluation in humans. *J. Control. Release* 89 (3), 419–428.
 Jayaraman, M.S., Bharali, D.J., Sudha, T., Mousa, S.A., 2012. Nano chitosan peptide as a potential therapeutic carrier for retinal delivery to treat age-related macular degeneration. *Mol. Vis.* 18, 2300–2308.
 Ko, J.A., Park, H.J., Hwang, S.J., Park, J.B., Lee, J.S., 2002. Preparation and characterization of chitosan microparticles intended for controlled drug delivery. *Int. J. Pharm.* 249, 165–174.
 Kreuter, J., 1993. Particulates (nanoparticles and microparticles). In: Mitra, A.K. (Ed.), *Ophthalmic Drug Delivery Systems*. Marcel Dekker, New York, pp. 275–297.
 Mi, F.L., Sung, H.W., Shyu, S.S., Su, C.C., Peng, C.K., 2003. Synthesis and characterization of biodegradable TPP/genipin co-crosslinked chitosan gel beads. *Polymer* 44 (21), 6521–6530.
 Mishra, G.P., Bagui, M., Tamboli, V., Mitra, A.K., 2011. Recent applications of liposomes in ophthalmic drug delivery. *J. Drug Deliv.* 2011, 1–14.
 Nagarwal, R.C., Kumar, R., Dhanawat, M., Pandit, J.K., 2011. Modified PLA nano in situ gel: a potential ophthalmic drug delivery system. *Colloids Surf. B Biointerfaces* 186 (1), 28–34.
 Patel, A., Cholkar, K., Agrahari, V., Mitra, A.K., 2013. Ocular drug delivery systems: an overview. *World J. Pharmacol.* 2 (2), 47–64.
 Patravale, V.B., Kulkarni, R.M., 2004. Nanosuspensions: a promising drug delivery strategy. *J. Pharm. Pharmacol.* 56, 827–840.
 Peptu, C.A., Buhus, G., Popa, M., Perichaud, A., Costin, D., 2010. Double cross-linked chitosan–gelatin particulate systems for ophthalmic applications. *J. Bioact. Compat. Polym.* 25 (1), 98–116.
 Quan, D.T., Le Bloa, A., Habib, H., Bonnaud, O., Meinel, J., Quemerais, A., Marchand, R., 1989. Couches minces d'oxynitride de phosphore. Application aux structures MIS sur InP. *Rev. Phys. Appl.* 24, 545–551.
 Riley, G.P., Harrall, R.L., Watson, P.G., Cawston, T.E., Hazleman, B.L., 1995. Collagenase (MMP-1) and TIMP-1 in destructive corneal disease associated with rheumatoid arthritis. *Eye* 9, 703–718.
 Scofield, J.H., 1976. Slater subshell photoionization cross-sections at 1254 and 1487 V. *J. Electron Spectrosc. Relat. Phenom.* 8, 129–137.
 Seng, W.L., Glogowski, J.A., Wolf, G., Berman, M.B., Kenyon, K.R., Kiorpes, T.C., 1980. The effect of thermal burns on the release of collagenase from corneas of vitamin A-deficient and control rats. *Invest. Ophthalmol. Vis. Sci.* 19, 1461–1470.
 Shirley, D.A., 1972. High-resolution X-ray photoemission spectrum of the valence bands of gold. *Phys. Rev. B* 5, 4709–4714.
 Shu, X.Z., Zhu, K.J., 2002a. Controlled drug release properties of ionically cross-linked chitosan beads: the influence of anion structure. *Int. J. Pharm.* 233, 217–225.
 Shu, X.Z., Zhu, K.J., 2002b. The influence of multivalent phosphate structure on the properties of ionically cross-linked chitosan films for controlled drug release. *Eur. J. Pharm. Biopharm.* 54 (2), 235–243.
 Silva, R.M., Silva, G.A., Coutinho, O.P., Mano, J.F., Reis, R.L., 2004. Preparation and characterisation in simulated body conditions of glutaraldehyde crosslinked chitosan membranes. *J. Mater. Sci. Mater. Med.* 15, 1105–1112.

Trivedi, R., Kompella, U.B., 2010. Nanomicellar formulations for sustained drug delivery: strategies and underlying principles. *Nanomedicine* 3, 485–505.

Wagh, V.D., Apar, D.U., 2014. Cyclosporine A loaded PLGA nanoparticles for dry eye disease: in vitro characterization studies. *J. Nanotechnol.* 10 Article ID 683153.

Wagner, C.D., Naumkin, A.V., Kraut-Vass, A., Alisson, J.W., Powell, C.J., Rumble Jr, J.R., 2003. NIST-X-ray Photoelectron Spectroscopy Database 20 Version 3.4. National Institute of Standards and Technology, Gaithersburg, MD, pp. 3.

Wagner, C.D., Riggs, W.M., Davis, L.E., Moulder, J.F., 1979. Handbook of X-ray photoelectron spectroscopy. In: Muilenberg, G.E. (Ed.), Eden Prairie, Minnesota.